Cell. Mol. Life Sci. (2016) 73:4559–4575
DOI 10.1007/s00018-016-2288-9

Cellular and Molecular Life Sciences

ORIGINAL ARTICLE

Novel nuclear hENT2 isoforms regulate cell cycle progression via controlling nucleoside transport and nuclear reservoir

Natalia Grañé-Boladeras[1,2,3] · Christopher M. Spring[4] · W. J. Brad Hanna[5] · Marçal Pastor-Anglada[1,2] · Imogen R. Coe[3]

Received: 19 January 2016 / Revised: 26 May 2016 / Accepted: 31 May 2016 / Published online: 6 June 2016

Abstract Nucleosides participate in many cellular processes and are the fundamental building blocks of nucleic acids. Nucleoside transporters translocate nucleosides across plasma membranes although the mechanism by which nucleos(t)ides are translocated into the nucleus during DNA replication is unknown. Here, we identify two novel functional splice variants of equilibrative nucleoside transporter 2 (ENT2), which are present at the nuclear envelope. Under proliferative conditions, these splice variants are up-regulated and recruit wild-type ENT2 to the nuclear envelope to translocate nucleosides into the nucleus for incorporation into DNA during replication. Reduced presence of hENT2 splice variants resulted in a dramatic decrease in cell proliferation and dysregulation of cell cycle due to a lower incorporation of nucleotides into DNA. Our findings support a novel model of nucleoside compartmentalisation at the nuclear envelope and translocation into the nucleus through hENT2 and its variants, which are essential for effective DNA synthesis and cell proliferation.

Keywords Nucleoside transporters · ENT2 · HNP36 · *SLC29A2* · Cell cycle regulation · DNA synthesis · Nucleoside metabolism

Abbreviations

CHX	Cycloheximide
ER	Endoplasmic reticulum
hCNT	Human concentrative nucleoside transporter
hENT	Human equilibrative nucleoside transporter
INM	Inner nuclear membrane
NCX	Sodium–calcium exchanger
NE	Nuclear envelope
NMD	Nonsense-mediated decay
NPC	Nuclear pore complex
NT	Nucleoside transporter
ONM	Outer nuclear membrane
ORF	Open reading frame
PPI	Protein–protein interaction
PP1	Protein phosphatase 1
PTC	Premature termination codon
TMD	Transmembrane domain
WT	Wild type

M. Pastor-Anglada and I. R. Coe are co-senior authors.

Electronic supplementary material The online version of this article (doi:10.1007/s00018-016-2288-9) contains supplementary material, which is available to authorized users.

✉ Natalia Grañé-Boladeras
nataliagrane@ryerson.ca

[1] Department of Biochemistry and Molecular Biology, Institute of Biomedicine (IBUB), University of Barcelona, 08028 Barcelona, Spain

[2] Oncology Program, CIBER EHD, Instituto de Salud Carlos III, 28029 Madrid, Spain

[3] Department of Chemistry and Biology, Ryerson University, Toronto, ON M5B 2K3, Canada

[4] Research Core Facilities, Keenan Research Centre, Li Ka Shing Knowledge Institute, Saint Michael's Hospital, Toronto, ON M5B 1T8, Canada

[5] Department of Biomedical Sciences, Ontario Veterinary College, University of Guelph, Guelph, ON N1G 2W1, Canada

Introduction

The cell cycle consists of a complex series of coordinated processes that ensure correct development and growth of tissues. Regulation of cell cycle is foundational to all aspects of normal cell functioning and its dysregulation contributes to many diseases. Therefore, enhanced insights into the mechanisms involved in cell cycle regulation are fundamental to understanding all aspects of cell physiology in health and disease. DNA replication is a key event during cell cycle progression [1–3]. Nuclear DNA replication is a tightly controlled process which ensures a faithful copying of the genome during each cell cycle [4, 5]. This complex process requires the participation of many protein complexes and enzymes [4, 6] and an essential element is the availability of a substantial and accessible pool of nucleotide building blocks for DNA synthesis [7]. Surprisingly, the location, source and regulation of these critical pools of nucleotides within the cell are not well known despite their essential role in cellular proliferation. It has been clearly demonstrated that insufficient supply of nucleotides during DNA replication results in slow replication fork progression resulting in DNA damage and genomic instability [7, 8]. These data suggest that an enhanced understanding of the factors that regulate and maintain pools of nucleotides will provide insight into the regulation of DNA replication and cellular proliferation.

Nucleotides are phosphorylated nucleosides, which are either synthesised in the cytosol through the energetically demanding de novo synthesis pathway, or are acquired by the cell from extracellular sources via the salvage pathway [9–11]. Nucleosides are hydrophilic and, therefore, require specialised integral membrane transport proteins, known as nucleoside transporters (NT) for transmembrane flux [12, 13]. The NTs comprise two non-homologous solute carrier families, SLC28, encoding human concentrative nucleoside transporters (hCNTs) and SLC29, encoding human equilibrative nucleoside transporters (hENTs) [12–14]. Both families have been traditionally regarded as being predominantly plasma membrane transporters [15]. However, prior to the cloning of the first member of the SLC29 gene family (hENT1) [16], a novel nuclear protein named HNP36 was identified in fibroblasts as a mitogenic delayed-early response gene [17] and was subsequently confirmed as a splice variant of hENT2 [18]. The physiological significance of this observation was not investigated further although the existence of functional nuclear hENTs in human cells was reported [19]. Taken together, these data suggest a previously unidentified, but potentially essential, nuclear role for ENTs in contributing to the regulation and supply of essential ingredients for DNA synthesis, and thus cellular proliferation.

The mechanisms that regulate supply of DNA building blocks to the nucleus are not well understood. Nucleos(-t)ides are compartmentalised into cytoplasmic and nuclear pools in the cell and these pools are in disequilibrium with each other, such that concentrations in the cytosol and the nucleus vary depending on the needs of the cell [20–22]. Insufficient nuclear pools of nucleotides during DNA replication result in dysfunctional cell proliferation [7, 8]. Therefore, we propose that NTs participate in the nucleoside compartmentalisation and are key contributors to effective proliferative function in human cells. We present here evidence for the existence and presence of two novel functional isoforms of hENT2 at the nuclear envelope, which possess a previously unidentified role in cell cycle progression. We propose a novel model of nucleoside processing at the nuclear envelope, which enables the rapid deployment of nucleotides into the nucleus during DNA replication and which is essential for cell proliferation.

Materials and methods

Cell culture, transfection and MTT assay

HEK-293 (ATCC—CRL 1573) and HeLa (ATCC—CCL-2) cells were maintained in proliferative conditions in Dulbecco's Modified Eagle's Medium (DMEM) with 4.5 mg/ml glucose and supplemented with 10 % (v/v) Foetal Bovine Serum (FBS) (Gibco) at 37 °C in a humidified incubator and a 5 % CO_2 atmosphere. Both cell lines were certified to be mycoplasma free by an external agency (DDC Medical). When indicated, cells were transiently transfected according to the manufacturer's instructions, using Lipofectamine® 2000 (Invitrogen) for hENT2 and hENT2-related constructs and Lipofectamine® 3000 (Invitrogen) for transfecting shRNA constructs, obtaining transfection efficiencies of approximately 60–70 %. Protein extraction, confocal microscopy and nucleoside transport assays were carried out 36 h after transfection and knockdown experiments were analysed at 72 h post-transfection.

For viability assays, HEK-293 cells were seeded in 96-well plates and transfected with different combinations of shRNA constructs. At 72 h post-transfection, MTT (3-(4,5-dimethylthiazol-2-yl)-2,5-diphenyltetrazolium bromide) dissolved in non-supplemented culture medium was added to a final concentration of 0.75 mg/ml and cells were incubated at 37 °C for 30 min. Cell respiration leads to an insoluble purple formazan product being formed in living

cells. MTT solution is removed at 30 min and DMSO (100 µl) was added to each well to solubilise the formazan product. Absorbency of the resulting solution was determined using a plate reader at 550 nm wavelength. Results were normalised to samples transfected with scrambled shRNA (control) set to 100 % viability.

Cloning of hENT2 and hENT2 splice variants, HA-tagged and shRNA constructs

The full ORF of hENT2 was amplified by polymerase chain reaction (PCR) using PfuTurbo® DNA high-fidelity polymerase (Roche) and four different batches of cDNA from the breast cancer cell line MCF7. Use of FL4F and FL5R primers (Table S4) resulted in the amplification of at least four different products ranging in size from 1000 to 1500 bp and which were visualised by electrophoresis in 1 % agarose gel. After gel extraction, hENT2 amplicons were ligated into the vector pGemT Easy (Promega) and transformed into competent *E. coli* DH5α bacteria (Invitrogen). Cloning resulted in a total of 360 colonies, which were screened by PCR. 110 clones were isolated and further sequenced, resulting in a total of 33 clones which were all confirmed to be the full-length WT hENT2 isoform, while 77 were splice variants of hENT2.

Isoforms 10C, 4A, 16D and 45F were sub-cloned into *Apa*I and *Pst*I sites of the mammalian expression vector pcDNA3.1 (Invitrogen). The epitope tag HA (YPYDVPDYA) was inserted at the C terminus of hENT2 and hENT2 splice variants by three sequential steps of site-directed mutagenesis PCR using PfuTurbo® polymerase (Roche), inserting nine extra nucleotides in each reaction. Primers used for HA insertion are listed in Table S4. Full-length WT hENT2 was further cloned into *Kpn*I and *Xba*I sites of the mammalian expression vector p3xFLAG-CMV-7.1 (Sigma-Aldrich). The 3xFLAG-hENT1 construct was previously generated in Dr. Coe's lab.

The shRNA constructs were specifically designed to target the exon 1–exon 3 junction in the case of 197J—lack of exon 2, which includes variants 4A (HNP36) and 45F (HNP32) and the exon 3–exon 5 junction in the case of 198J—lack of exon 4, which includes variants 16D and 45F (both codifying HNP32). Both sequences are listed in Table S4. shRNA constructs were customised and cloned into psi-U6.1 vector from GeneCopoeia (http://www.genecopoeia.com), which includes eGFP sequence as reporter gene. The control used consisted of a scrambled shRNA construct and was provided by the same company (GeneCopoeia).

mRNA surveillance test and qPCR analysis

Eukaryotic cells possess a nonsense-mediated decay (NMD) pathway, which detects and degrades mRNA transcripts that contain premature termination codons (PTC). The NMD pathway is linked to the synthesis of proteins as it detects the PTC once the ribosome binds to the mRNA and the translation starts [23].

To determine if mRNA is degraded by the NMD pathway, HEK-293 cells were treated with 20 µg/ml CHX (Sigma-Aldrich) in non-supplemented DMEM for 6 h at 37 °C. CHX inhibits protein biosynthesis, which is required by the NMD pathway consequently inhibited by the treatment. Total RNA was extracted using PureLink® RNA mini kit (Ambion) and cDNA was synthesised using SuperScript® III First Strand Synthesis Kit (Invitrogen) according to manufacturer's instructions. A positive control for this approach consisted of amplification of the nPTB gene, which has been previously describe to undergo the NMD pathway [24], by PCR and followed by analysis by agarose gel as previously described [24]. Results confirmed an increase of the exon 10-skipped variant of nPTB proving the NMD pathway was blocked by CHX treatment. Relative quantitative analysis of mRNA expression (real-time PCR or qPCR) was performed using SYBER® Green PCR Master Mix and 7500 Fast Real-time PCR system (Applied Biosystems). Primers designed for qPCR (Table S4) were initially validated and amplification efficiencies were confirmed to be between 90 and 110 %. Combinations of four different primers allowed specific amplification of each one of the hENT2 isoforms under study. GAPDH was used as a housekeeping gene and nPTB as a positive control. Results were calculated by normalising treated samples to their untreated controls using the formula $2^{-\Delta\Delta C_t}$. The same protocol and primers were used to confirm knockdown of hENT2 isoforms after transfection of shRNA constructs with the exception of HMBS and HPRT1 as housekeeping genes.

qPCR screening for hENT2 and hENT2 splice variants was conducted using a commercial multiple tissue and cell line panel (Clontech). Samples used in the panel are reported to come from human tissues and cancer cell lines free of genomic DNA. The same previous primers were used for individual amplification of the different hENT2 isoforms and housekeeping genes. Amplification of total hENT2 mRNA (including full-length and splice variants) was conducted using primers F0 and R0 (Table S4) for comparison. For the results, all samples were normalised to total hENT2 in HEK-293, using the formula $2^{-\Delta\Delta C_t}$.

SDS-PAGE and immunoblotting analysis, co-immunoprecipitation and confocal microscopy

Since well-validated, highly specific antibodies against hENT2 splice variants are not available, we conducted immunoblotting and immunocytochemistry using HA antibodies against HA-tagged constructs of hENT2 and hENT2 splice variants. Briefly, HEK-293 cells were transiently transfected for 36 h with hENT2-HA and hENT2-HA splice variants followed by extraction of total protein using NP-40 lysis buffer (Tris–HCl 50 mM pH8, NaCl 150 mM, Nonidet P40 1 % (v/v), $Na_4P_2O_7$ 5 mM, NaF 50 mM, Na_3VO_4 1 mM and protease inhibitor cocktail; cOmplete Mini—Roche). Protein extracts were quantified using Bradford protein assay kit (Bio-Rad). When indicated, protein extracts were incubated with PNGase F (New England Biolabs), an amidase that cleaves between the innermost GlcNAc and asparagine residues of oligosaccharides from N-linked glycoproteins, following the manufacturer's instructions. Denatured protein extracts (30 μg of protein for 30 min at 37 °C in presence of β-mercaptoethanol) were separated in 12 % (v/v) SDS–polyacrylamide gels by electrophoresis (SDS-PAGE) and transferred to nitrocellulose membranes (Bio-Rad). Following incubation with anti-HA High-Affinity Antibody (diluted 1:2000; Roche) and polyclonal anti-ENT2 antibody (diluted 1:1000; Abcam), proteins were detected using a secondary antibody conjugated to horseradish peroxidase and an enhanced chemiluminescence detection kit (Thermo Scientific). For co-immunoprecipitation experiments, HEK-293 cells were co-transfected with combination of one HA-tagged protein as bait, HNP36 (4A-HA) or HNP32 (45F-HA) and one Flag-tagged protein as prey (either Flag-hLa as negative control, Flag-hENT1 or Flag-hENT2). Total protein was extracted with NP-40 buffer and incubated with HA-affinity columns from Pierce HA Tag IP/Co-IP Kit (Thermo Fischer), following the manufacturer's protocol. Results were visualised by SDS-PAGE as previously described.

To determine the sub-cellular localization of each isoform, immunocytochemistry and confocal microscopy of hENT2 and hENT2 variant HA-tagged proteins were performed on semiconfluent monolayers of transiently transfected HEK-293 cells cultured on glass coverslips. Cells were treated with CHX (10 μg/ml) in non-supplemented DMEM for 3 h at 37 °C to reduce protein background at the ER. Glass coverslip-grown transfected cells were incubated for 15 min in 3 % (w/v) paraformaldehyde in phosphate-buffered saline (PBS), rinsed 3 times in PBS, incubated with 10 % (v/v) FBS in PBS for 30 min, incubated with anti-HA (diluted 1:200; Roche), anti-NPC (diluted 1:500; Abcam) and/or anti-Flag (diluted 1:500; Sigma-Aldrich) for 1 h at room temperature, rinsed three times with PBS, incubated with secondary antibodies Alexa® 555 Donkey anti-Mouse and Alexa® 488 Donkey anti-Rat (both diluted 1:300, Invitrogen), rinsed three times with PBS, incubated with DAPI 3 nM in PBS for 5 min when indicated, rinsed three more times with PBS and mounted on slides using aqua-based mounting medium (MP Biomedicals). Images were obtained using the Olympus Fluoview 300 confocal microscope and analysed with Olympus Fluoview 300 Imaging software under blind observation to preserve an objective perception. All the confocal images show a single and representative section of a Z-series taken through the entire cell.

Nucleoside and nucleobase transport assays

Transport studies on monolayer-cultured cells were carried out as previously described [25] by exposing replicate cultures at room temperature to the appropriate ^{3}H-labelled nucleoside or nucleobase (1 μM, 1 μCi/ml) in uptake buffer (5.4 mM KCl, 1.8 mM $CaCl_2$, 1.2 mM $MgSO_4$, 10 mM HEPES and 137 mM choline chloride) supplemented with 1 μM NBTI (hENT1 inhibitor—A) or 10 μM dipyridamole (hENT1 and hENT2 inhibitor—B) or nothing (hENT1 + hENT2 activity plus diffusion—C). Incubation was stopped after 10 s by washing the monolayers three times in cold uptake buffer supplemented with NBTI and dipyridamole. hENT-specific transport rates were calculated as follows: hENT1 = C − A; hENT2 = C − hENT1 − B.

Xenopus laevis oocytes were used for heterologous hENT2 and hENT2 splice variants activity assays since they lack endogenous nucleoside transport activity [26] and, for reasons that remain unclear, intracellular nucleoside transporters are trafficked to the plasma membrane in *Xenopus* oocytes, allowing detailed and extensive functional characterization [27, 28]. Oocytes were removed from adult female frogs in accordance with an animal utilisation protocol approved by the Animal Care Committee, University of Guelph. After extraction, stage V–VI oocytes were stored overnight at 18–20 °C in ND96 medium (NaCl 96 mM, KCl 2 mM and HEPES 5 mM supplemented with gentamicin sulphate (50 μg/ml), penicillin G (100 μg/ml), pyruvic acid 2 mM, theophylline 90 mg, $MgCl_2$ 1 mM and CaCl2 1.8 mM). Follicle layers were removed by treating the oocytes with collagenase Type I (1 mg/ml) for 20–40 min in calcium-free saline. cRNA samples were generated according to mMessage mMachine® Kit manufacturer's protocol (Ambion) and validated by 2100 Bioanalyzer (Agilent Technologies). cRNA (75 ng/oocyte) was injected into 15–20 oocytes per condition per trial using a nanoinjector. Following injection, oocytes were kept at room temperature for 72 h in ND96 medium, changing to fresh medium daily. To asses

transport activity, oocytes were incubated for 60 min at room temperature in choline chloride transport buffer (200 µl) containing 10 µM of un-labelled substrate and 0.1 mCi/ml of ^{3}H-labelled substrate. Following incubation, extracellular substrate was removed using three rapid washes (1 ml) with ice-cold choline chloride buffer containing 10 µM dipyridamole. Each single oocyte was then placed into a separate scintillation vial with 1 % (v/v) SDS (200 µl). Vials were subjected to vigorous shaking for 45 min before addition of scintillation fluid and counting.

Flow cytometry: apoptosis, proliferation and cell cycle

Flow cytometry data were analysed using a MACSQuant® Analyzer (MiltenyBiotec) at the Research Core Facilities of Saint Michael's Hospital in Toronto. To determine the apoptotic status of samples, cells were seeded and transfected with shRNA constructs targeted against 4A (HNP36—197J shRNA), 16D (HNP32—198J shRNA) and 45F (HNP32—197J and 198J shRNAs). The shRNA constructs co-expressed GFP and thus cytometric analyses in knockdown experiments were limited to GFP-positive cells. At 72 h post-transfection, cells were liberated using trypsin, inactivated through the addition of supplemented media, pelleted at 500*g* for 5 min, resuspended in 0.5 ml of Annexin V binding buffer and 25 µl of Annexin V (Life Technologies) and incubated on ice for 15 min. Cells were then co-stained with 1 µg/ml of propidium iodide and analysed by flow cytometry.

For cell proliferation assays, cells were labelled with 10 µM CellTrace Violet (Life Technologies) for 10 min according to the previously published method [29]. 48 h post-labelling, samples were trypsinised as described above and analysed via flow cytometry and proliferative capacity and generation peaks modelled using FCS Express version 4 (De Novo Software). In both cases, manufacturer's protocols were followed and samples were positively gated based on high GFP expression and single events during the analysis. To analyse cell cycle we conducted a one-dimensional determination of DNA content using propidium iodide as previously described [30] and results were analysed with an FCS express 4.0 multicycle DNA fitting algorithm with G1 CVs of <4 %.

Thymidine incorporation into DNA, nuclei isolation and fractioning

To quantify thymidine incorporation into DNA and presence in the nuclei, we used two different protocols. First, cells were seeded in 100 mm plates and incubated with 1 µCi/mL of [^{3}H]-thymidine for 2 h after 72 h of knockdown of HNP36 and HNP32 with the co-expression of shRNA constructs 197J + 198J. Cells were then fixed in ice-cold 70 % methanol, washed in ice-cold 3 % trichloroacetic acid (TCA) and solubilised 1 % SDS and 0.3 % NaOH. Samples contained nuclear radio-labelled thymidine, either incorporated into DNA or stored in the nuclear envelope. Radioactivity was counted by liquid scintillation using a standard scintillation counter [31]. The second protocol used to quantify nuclear thymidine was based on nuclei isolation and fractioning. Nuclei were isolated using the commercial Nuclei Isolation Kit (Sigma-Aldrich) following the manufacturer's instructions. Samples were split into two and one half was resuspended in 1 % SDS and 0.3 % NaOH, added scintillation liquid and counted with the scintillation counter. The rest of each sample was fractioned into the inner nuclear membrane (INM) and the outer nuclear membrane plus lumen (ONM). For this, samples were incubated with a 1 % citric acid solution on ice for 15 min and pelleted at 5000×*g* for 10 min [32]. Pellets contain the inner nuclear membranes and the nucleoplasm (INM) and supernatants the outer nuclear membrane and the nuclear lumen (ONM). Both fractions were resuspended in 1 % SDS and 0.3 % NaOH, added scintillation liquid and counted with the scintillation counter. When indicated, cells were arrested after 24 h of serum and amino acid starvation (non-supplemented MEM medium) [33].

Results

Novel splice variants of hENT2 identified in MCF7 cells

Full-length wild-type (WT) hENT2 (GenBank: NM001532) and splice variants were cloned as described in the "Materials and methods". The splice variants were classified and compared based on the putative proteins generated by their open reading frames (ORFs) (Table S1). Two variants, 22C (Genbank: AF401235) and 17G (GenBank: BC011387), are predicted to generate proteins containing the first six transmembrane domains (TMD) of the full-length hENT2 protein. Variant 22C has been previously described as hENT2A and which is located in an intracellular location with a vesicular distribution [34]. Due to the similarity in the predicted structure of 22C and 17G, we hypothesised that the isoform 17G was a new cytoplasmic variant.

We also identified a variant, 22E, which lacks 68 nucleotides in exon 4, resulting in a translated protein of 36 kDa and which has been previously described as a hydrophobic nucleolar protein (HNP36; GenBank: X86681) comprising 326 amino acids [17]. However, more extensive bioinformatic analysis using current nucleic acid

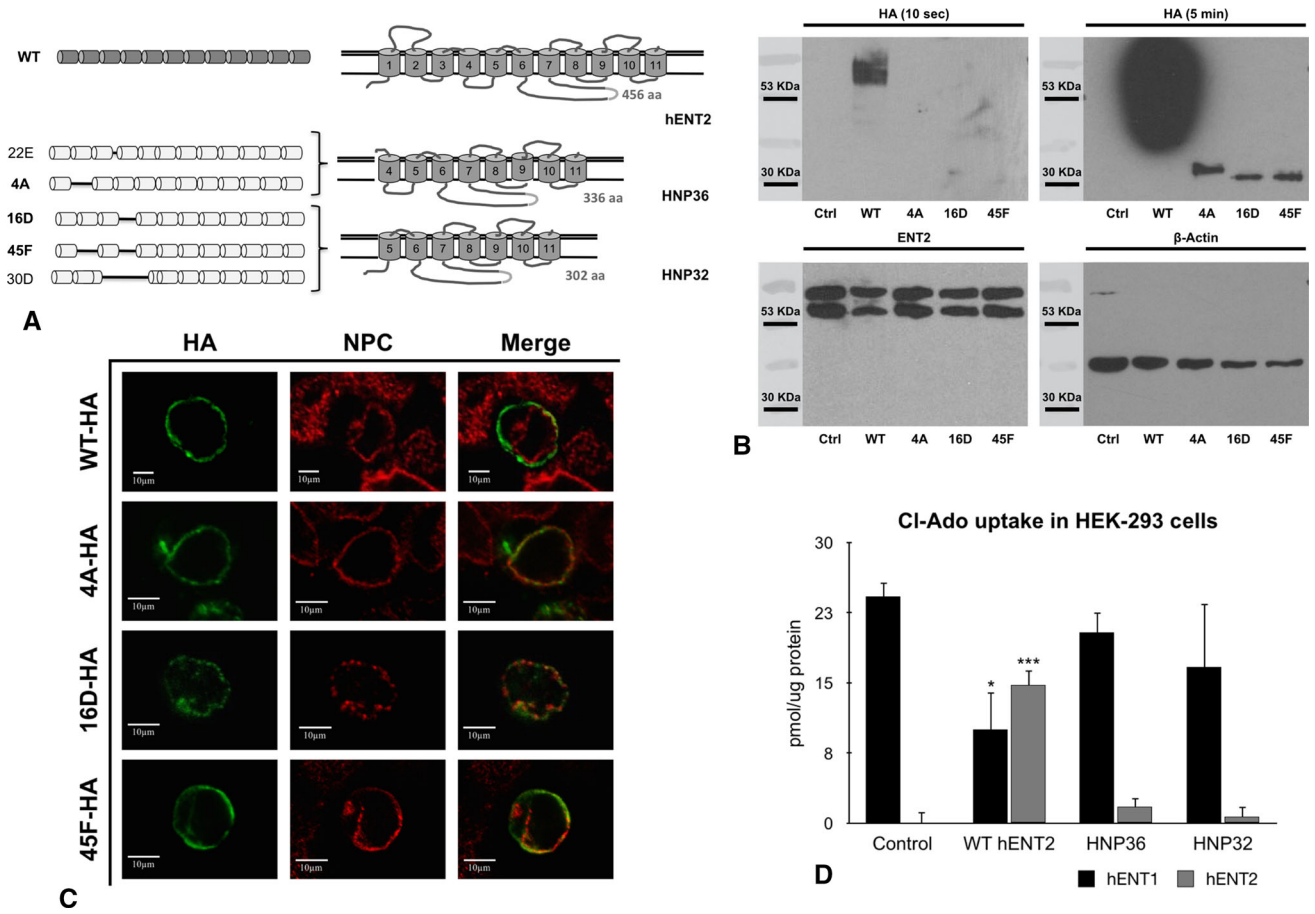

Fig. 1 Nuclear splice variants of hENT2. **a** Structure of hENT2 and hENT2 splice variant transcripts (*left*) and putative proteins (*right*). Further studies were conducted using WT, 4A, 16D and 45F isoforms. See also Figure S1 and Tables S1, S2 and S3. **b** Immunoblots of endogenous hENT2 and overexpressed hENT2-HA proteins (WT 10C-HA; 4A-HA; 16D-HA and 45F-HA) obtained from HEK-293 cells. Control samples were transfected with empty pcDNA3.1 vector. *Top* membranes were incubated with anti-HA antibody and films were exposed for 10 s (*top left*) or 5 min (*top right*). Short exposure revealed two bands of WT hENT2-HA above 53 kDa, whereas longer exposure showed HNP36 and HNP32 bands above 30 kDa. Membranes incubated with anti-ENT2 antibody (*bottom left*) showed WT hENT2 double band at 55 and 60 kDa in all samples but could not detect overexpressed splice variants. β-Actin (*bottom right*) was used as loading control (representative image; $n = 7$). **c** Confocal microscopy of HEK-293 cells expressing hENT2-HA proteins (*green*) and nuclear envelope marker nuclear pore complex (NPC; *red*). WT hENT2 does not co-localise with NPC whereas 4A-HA, 16D-HA and 45F-HA co-localise with NPC at the nuclear envelope (representative image; $n = 6$). **d** Nucleoside uptake in HEK-293 cells expressing WT hENT2 and hENT2 nuclear variants. Non-transfected HEK-293 cells (control) show very little hENT2 activity whereas WT hENT2 transfected cells show significantly higher hENT2 activity. Cells transfected with either HNP36 (4A-HA) or HNP32 (45F-HA) did not show any significant changes in hENT2 activity compared to control cells (mean ± SD; $n = 3$; $*p < 0.05$, $***p < 0.001$)

sequence analysis programs suggests that this transcript results in a protein consisting of 336 amino acids. A novel splice variant (4A), lacking exon 2 and resulting in a predicted ORF of 336 amino acids, is identical to our prediction for HNP36 (Fig. 1a). Three more variants (16D, 45F and 30D) were cloned, each producing the same translated protein containing the last seven TMD of the WT protein. This structure consists of one less TMD than HNP36 and we anticipated this protein to be another nuclear isoform of hENT2.

We also identified three splice variants with deletions at each end of the transcript, which would result in small proteins of three TMD. We hypothesised it is unlikely that these variants would reach the plasma membrane or form functional proteins based on the extent of the truncations. Therefore, we focussed further analysis on the putative nuclear variants (4A, 16D and 45F) together with the WT isoform. Nucleic acid and protein sequences of 4A, 16D and 45F splice variants are listed in Tables S2 and S3.

Novel splice variants of hENT2 are functional transporters localised at the nuclear envelope (NE)

mRNA surveillance tests in HEK-293 cells confirmed that the splice variants 4A, 16D and 45F are endogenously expressed, validating that further observations in a

heterologous system are not artefacts of overexpression (Figure S1).

The molecular weights of the splice variant proteins (4A, 16D and 45F) are consistent with predicted ORFs (36 kDa for HNP36, and 32 kDa for a protein that we identified as HNP32) and contrasted with the typical doublet species (55 and 60 kDa) seen for the WT hENT2 (Fig. 1b). HA-tagged splice variant proteins are present at the nuclear membranes based on their co-localisation with nuclear pore complex (NPC) (Fig. 1c). Lack of functional transport at the plasma membrane by the splice variants (in contrast to WT hENT2-dependent uptake) in HEK-293 cells (Fig. 1d) confirmed that these variants were not present at the plasma membrane, as we previously observed (Fig. 1c). Intriguingly, hENT1-dependent nucleoside uptake decreased significantly when WT hENT2 was overexpressed suggesting that relative abundance of hENT1/2 isoforms at the plasma membrane impacts overall nucleoside transport.

While the splice variants do not contribute to plasma membrane nucleoside flux, they do transport nucleosides (purine, pyrimidine; Fig. 2a, b) and nucleobases (Fig. 2c) when expressed heterologously in *X. laevis* oocytes, thereby proving they are functional transporters as anticipated by previous structural studies on ENT-like proteins [35, 36]. Our analysis demonstrates that all splice variants have transport profiles similar to full-length hENT2, except for HNP36, which shows slightly increased nucleoside uptake.

hENT2 nuclear variants are highly expressed in cancer cells compared to healthy tissue

Alternative splicing is highly regulated in cell proliferation and its dysregulation results in serious diseases such as cancer [37–40]. Since HNP36 was initially identified as a delayed-early response gene for which expression increases after mitogenic stimuli [17], we hypothesised that generation of nuclear hENT2 variants is also regulated and that these variants would be preferentially expressed under proliferative conditions.

Full-length WT hENT2 is the predominant species expressed in a broad range of human tissues and cell lines

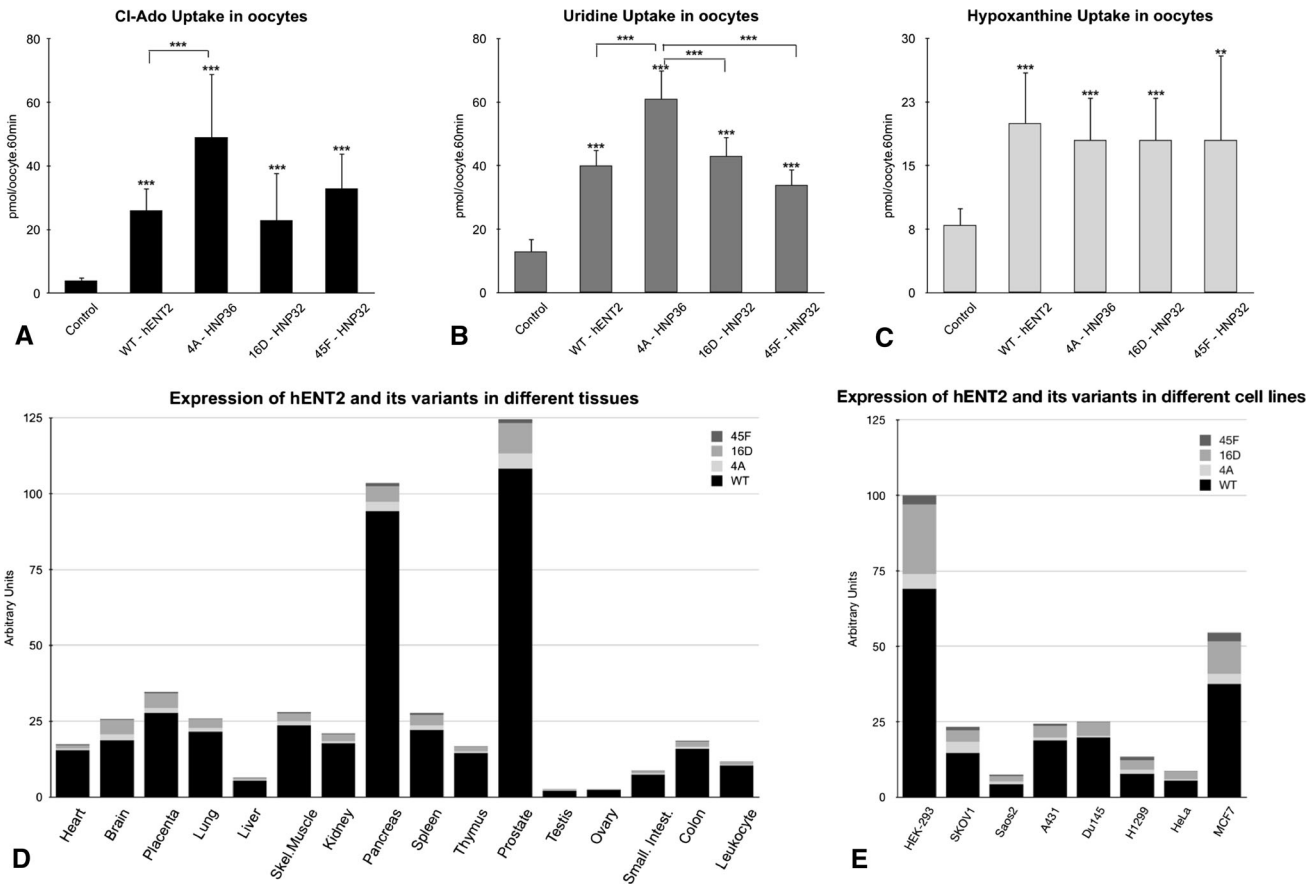

Fig. 2 Activity and expression profiles of hENT2 nuclear variants. **a** 2-Chloro-adenosine, **b** uridine and **c** hypoxanthine uptake in *X. laevis* oocytes expressing hENT2 nuclear variants. HNP36 and HNP32 are functional nucleoside and nucleobase transporters when expressed in *X. laevis* oocytes (mean ± SEM; $n = 10$–15; $^{**}p < 0.01$, $^{***}p < 0.001$). **d** mRNA expression levels of hENT2 isoforms in different human tissues and **e** cell lines

(Fig. 2d, e) although total levels of mRNA expression and overall proportions of each splice variant vary among tissues (Fig. 2d) and cell lines (Fig. 2e). In human tissues, full-length hENT2 represents 80–90 % of the total mRNA hENT2 expression but only 55–80 % in cancer cell lines. Splice variants have lower mRNA expression levels in normal tissue but these levels rise in proliferative cells in culture (e.g. 16D, <10 % of total hENT2 in healthy tissue vs. 15–30 % in cell lines).

Taken together, our results confirm that nuclear hENT2 splice variants are broadly expressed among different tissue types and cell lines and that highly proliferative cells (cancer cells) have higher mRNA expression levels of nuclear hENT2 isoforms compared to non-proliferative tissues. These results suggest that the regulation of alternative splicing of hENT2 is correlated with proliferative status of the cell leading us to speculate that nuclear hENT2 variants play a role in cell proliferation.

Nuclear variants of hENT2 recruit full-length isoform to the NE and form functional heteromers by protein–protein interaction (PPI)

Alternative splicing can regulate protein function [41] in a variety of ways, including a role for splice variants as dominant negative regulators of WT proteins by modifying sub-cellular localisation [42–45]. We predicted that nuclear hENT2 splice variants act as functional transporters at the NE and represent a novel mode of regulation of WT hENT2 by modifying localisation or functionality of the full-length protein depending on the proliferative needs of the cell.

Overexpression of hENT2-HA in HEK-293 cells confirmed the presence of the full-length protein at the plasma membrane but not at the NE (Fig. 1c), although a qPCR screen confirmed a high mRNA expression level of hENT2 nuclear variants in HEK-293 cells (Fig. 2e). However, overexpression of hENT2-HA increases the expression of WT hENT2 compared to the endogenous nuclear isoforms. Therefore, it would be very difficult to discern changes in localisation of WT hENT2 following this treatment. To confirm our hypothesis, we analysed sub-cellular localisation of WT hENT2 following co-transfection of both isoforms (Flag-hENT2 with HNP36-HA and HNP32-HA). Confocal microscopy confirmed that hENT2-HA (Fig. 1c) and Flag-hENT2 (Figure S2) are located at the plasma membrane when expressed alone in HEK-293 cells. However, Flag-hENT2 is present at the NE and co-localises with HNP36-HA (construct 4A-HA) or HNP32-HA (construct 45F-HA) when co-expressed in HEK-293 cells (Fig. 3a). Co-transfection of Flag-hENT1 with HNP36-HA and HNP32-HA showed co-localisation at the ER, where these proteins are synthesised, but failed to elicit the same alteration in sub-cellular distribution, suggesting this change is specific to hENT2 (Fig. 3a).

Fig. 3 Functional hENT2 heteromers at the nuclear envelope. ▶ **a** HEK-293 cells co-expressing Flag-hENT2 or Flag-hENT1 (*red*) with HA-tagged HNP36 (4A-HA) and HNP32 (45F-HA) (*green*). DNA was stained with DAPI (*blue*). hENT2 co-localises at the nuclear envelope with HNP36 and HNP32, unlike hENT1 which remains at the plasma membrane when co-expressed with HNP36 and HNP32 (representative images; $n = 3$). See also Figure S2. **b** Hypoxanthine hENT2-mediated and **c** 2-chloro-adenosine hENT1-mediated uptake in HeLa cells expressing different hENT2 isoforms. hENT2 transport activity at the plasma membrane significantly decreases after overexpression of HNP36 (4A), whereas hENT1 transport activity significantly decreases after hENT2 overexpression and increases after HNP36 overexpression (mean ± SD; $n = 3$; $^{*}p < 0.05$, $^{**}p < 0.01$). **d** Co-immunoprecipitation of Flag-hENT1 (E1) and Flag-hENT2 (E2) with HNP36-HA (4A-HA) and HNP32-HA (45F-HA). HNP32 and HNP36 protein–protein interact with hENT2 but not hENT1. Flag-hLa was used as negative control (representative image, $n = 4$). **e** 2-Chloro-adenosine and **f** hypoxanthine uptake in oocytes co-expressing WT hENT2 with HNP36 (4A) and HNP32 (45F) confirms that the transporters are functional when co-expressed in *X. laevis* oocytes (mean ± SEM; $n = 10$–20; $^{*}p < 0.05$, $^{***}p < 0.001$)

To determine if this change in sub-cellular localisation alters hENT2-dependent nucleoside uptake, we measured hypoxanthine and uridine transport in HeLa cells, which have endogenous hENT2 activity, and found that hENT2-mediated hypoxanthine transport was increased approximately twofold when WT hENT2 was overexpressed (Fig. 3b). In contrast, transfection of HNP36 (4A) resulted in a fourfold reduction in hENT2-mediated transport compared to control. These data are consistent with a model in which HNP36 mediate redistribution of hENT2 away from the plasma membrane and towards the NE. Endogenous hENT1-mediated uridine transport decreased (~threefold) following transfection with WT hENT2 (Fig. 3c). These results, together with the slight increase in hENT1-mediated uptake after transfection of HNP36, suggest that ENTs may compensate for each other in terms of activity when there are changes in the levels or presence of each isoform at the plasma membrane, as previously observed (Fig. 1d). These changes in hENT2-mediated uptake due to overexpression of HNP36, together with co-localisation of both proteins and altered hENT2 sorting inside the cell, suggest that hENT2 nuclear variants play a regulatory role in modulating presence and activity of full-length hENT2 at the plasma membrane.

Splice variants can regulate a WT protein via PPI [44–46]. We speculated that this was a mechanism of regulation of hENT2 and confirmed that HNP36-HA (4A-HA) and HNP32-HA (45F-HA) each co-immunoprecipitate with Flag-hENT2 (Fig. 3d), suggesting that the splice variants can interact with WT hENT2. The formation of PPI between WT hENT2 and its nuclear isoforms also

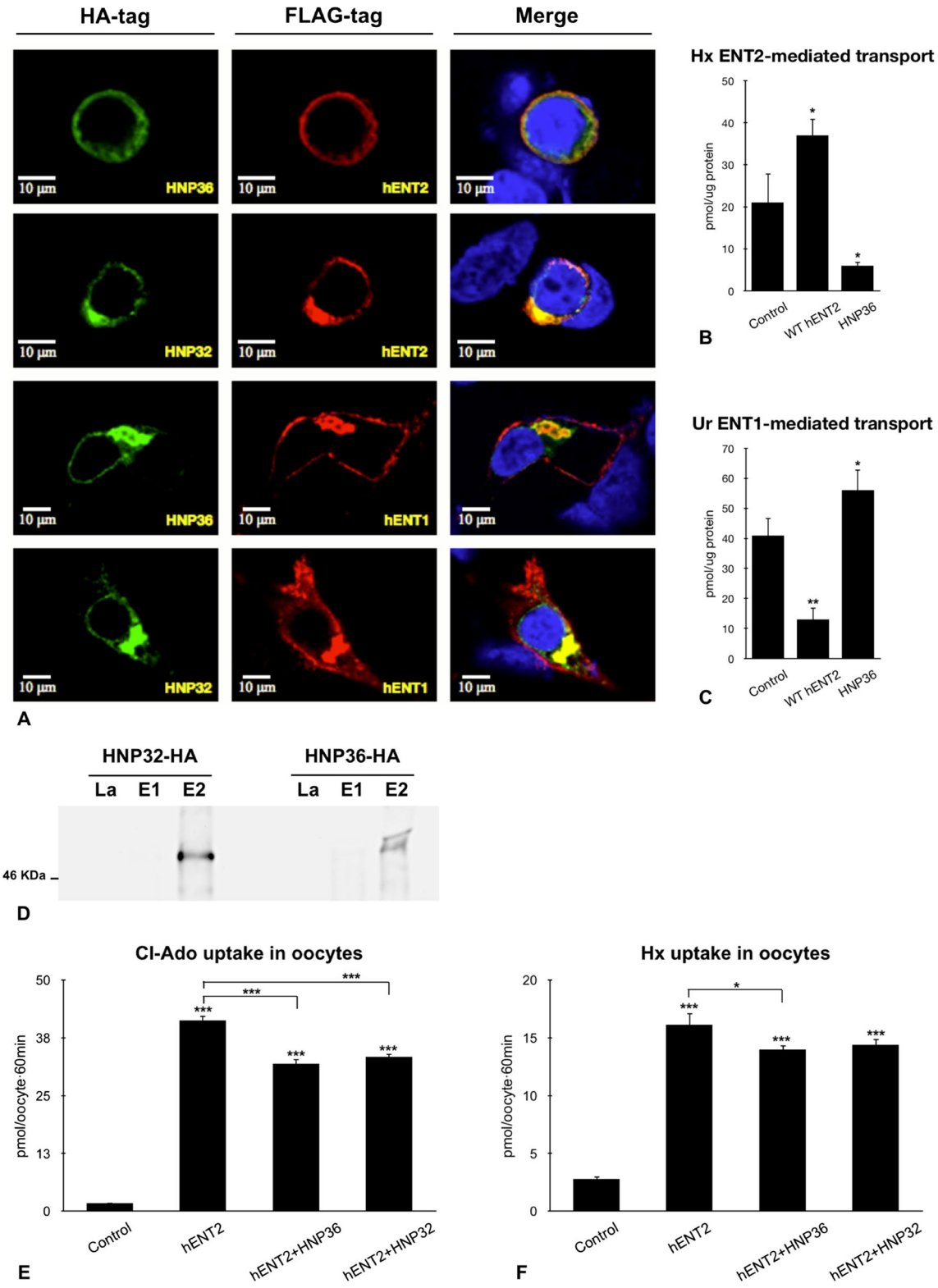
HA-tag
FLAG-tag
Merge
HNP36
hENT2
HNP32
hENT1
10 μm
A
Hx ENT2-mediated transport
pmol/ug protein
Control
WT hENT2
HNP36
B
Ur ENT1-mediated transport
C
HNP32-HA
HNP36-HA
La
E1
E2
46 KDa
D
Cl-Ado uptake in oocytes
pmol/oocyte·60min
hENT2+HNP36
hENT2+HNP32
E
Hx uptake in oocytes
F

suggests the presence of heteromers at the NE, which is supported by the observation that hENT1 did not co-immunoprecipitate with HNP36 or HNP32, proving these isoforms specifically interact with hENT2.

When HNP36 and HNP32 were co-expressed along with the WT hENT2 transporter protein in *X. laevis* oocytes, we observed that hENT2-mediated transport of 2-chloro-adenosine (Fig. 3e) and hypoxanthine (Fig. 3f) was slightly lower, although similar, compared to the transport observed when expressing WT hENT2 alone. These data are consistent with the concept that formation of hENT2–HNP36 and hENT2–HNP32 heteromers does not alter the basic functional properties of hENT2 proteins.

Knockdown of HNP36 and HNP32 leads to a decrease in cell proliferation and a dysregulation of cell cycle

We have shown here that hENT2 splice variants are broadly expressed among tissues and cell lines and that higher levels of expression are associated with proliferative conditions. Therefore, we hypothesised that HNP36 and HNP32, and the formation of functional hENT2 heteromers at the NE, contribute to cell proliferation by regulating nucleos(t)ide availability in the nucleus. Knockdown of HNP36 and HNP32 in HEK-293 cells was validated by qPCR analysis (Fig. 4a) and a decrease in HNP36 and HNP32 protein expression was later confirmed by Western blotting (Fig. 5c, d). The shRNA construct 197J targets those splice variants lacking exon 2, which are 4A (HNP36) and 45F (HNP32), whereas the targets for 198J shRNA construct are the variants lacking exon 4, which are 16D (HNP32) and 45F (HNP32). Knockdown of HNP36 and HNP32 in HEK-293 cells resulted in decreased cell survival (72 h post-transfection with shRNA constructs; Fig. 4b), which was enhanced by the presence of both constructs (197J < 198J < 197J + 198J). Since the effect on cell survival could be the result of changes in either cell proliferation or apoptosis, we analysed the apoptotic status of cells after knockdown of HNP36 and HNP32 (annexin V/PI staining of transfected cells; Figure S3) and observed no changes compared to control cells, suggesting the decrease in cell survival was due to changes in cell proliferation.

We confirmed a role for nuclear hENT2 splice variants in regulating cell proliferation by measuring the number of divisions that cellular populations of HEK-293 cells have undergone using a standard cellular flow cytometry-based proliferation assay. Following the knockdown of HNP36 and HNP32, we observed a decrease in cellular proliferation (average of number of replications per cell including undivided cells; Fig. 4c) and further confirmed that the decrease in cell proliferation was caused by a dysregulation in cell cycle since knockdown of HNP36 and HNP32 led to an increase in the number of cells in S phase (Fig. 4d) along with a decreased percentage of cells in G2 (Fig. 4e). We propose that this cell cycle arrest is due to an insufficiency in the nucleotide pools needed to sustain DNA replication, and the concomitant decrease in cell proliferation (Fig. 4f).

HNP36 and HNP32 recruit hENT2 to the inner nuclear membrane (INM) under proliferative conditions to supply nucleosides to the nucleus

To confirm that the dysregulation of cell cycle after HNP36 and HNP32 knockdown is caused by a decrease in nucleoside supply into the nucleus, we measured the incorporation of radio-labelled thymidine and thymidine metabolites into DNA in HEK-293 cells (Fig. 5a). Our results showed a 38 % decrease in thymidine incorporation after knockdown of HNP36 and HNP32 (co-transfecting both shRNA constructs 197J + 198J), suggesting that hENT2 splice variants are involved in the translocation of nucleosides into the nucleus. We measured a decrease (30–35 %) in thymidine incorporation into DNA in isolated nuclei (Fig. 5b) and the INM sub-fraction. There was also a marked decrease (40 %) in thymidine levels in the outer nuclear membrane (ONM) sub-fraction, which includes the lumen content, confirming the presence of nucleosides in the lumen of the NE and supporting our contention that nucleosides reach the nucleus across the ONM and INM via nucleoside transporters at the nuclear envelope.

Immunoblotting of isolated nuclei, INM and ONM sub-fractions from HEK-293 cells for hENT2 isoforms confirmed the presence of endogenous HNP36 and HNP32, visible as a double band (of slightly more than 30 kDa), in the total nuclei and INM fractions (Fig. 5c). As expected, the intensity of these bands decreased significantly (~65 %) after knockdown of HNP36 and HNP32 (Fig. 5d). Interestingly, WT hENT2 was present in all fractions although the lower molecular weight band was predominant at the INM while the larger molecular weight band was found predominantly at the ONM. ENTs are putatively glycosylated at their first extracellular loop and it has been reported that glycosylation could be involved in ENT's trafficking to the plasma membrane [47, 48]. We hypothesised that the lower molecular weight band observed for ENT2 could correspond to a deglycosylated form of the transporter. Total protein extracted from HEK-293 cells and incubated with PNGase F revealed no changes in size for the double band of hENT2, whereas Flag-hENT1 protein band decreased in weight after being deglycosylated (Fig. 5e). These results suggest that the difference between the two ENT2 protein bands would not be due to glycosylation.

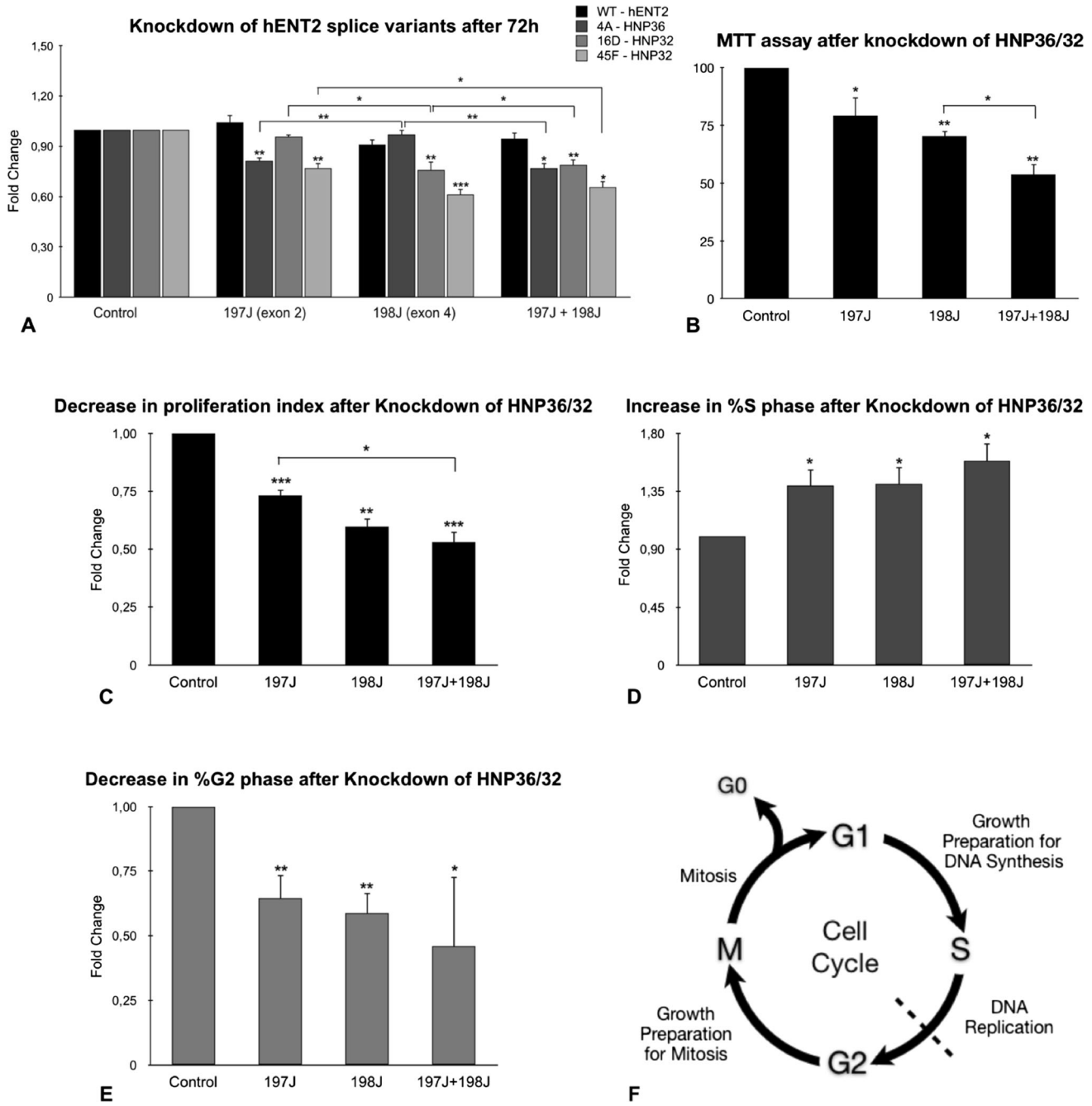

Fig. 4 Decrease in cell proliferation and dysregulation of cell cycle after knockdown of HNP36 and HNP32 in HEK-293 cells. **a** qPCR analysis of mRNA levels of hENT2 isoforms after 72 h of knockdown confirms a decrease in mRNA expression of HNP32 and HNP36. shRNA 197J targets splice variants 4A (HNP36) and 45F (HNP32) and shRNA 198J targets splice variants 16D (HNP32) and 45F. Control samples expressed a scrambled shRNA construct (mean ± SEM; $n = 3$–5). **b** MTT assays (mean ± SD; $n = 3$) and **c** proliferation assay (mean ± SEM; $n = 3$–5) after 72 h of knockdown. **d** Increase in %S phase (mean ± SD, $n = 3$) and **e** decrease in %G2 phase (mean ± SD; $n = 4$) after knockdown of hENT2 nuclear variants. **f** Schematic representation of cell cycle. See also Figure S3. $*p < 0.05$, $**p < 0.01$, $***p < 0.001$

Knockdown of HNP36 and HNP32 resulted in no overall changes in the total amount of hENT2 present at the nucleus, although there was approximately 40 % less at the INM (Fig. 5d). These results suggest that relative presence of HNP36 and HNP32 correlates with presence of WT hENT2 at the INM. To confirm that hENT2 is regulated by splice variants under proliferative conditions, we repeated the previous experiments using arrested cells after 24 h of starvation. Thymidine levels were decreased (∼17 %) in isolated nuclei in serum-deprived cells compared to control

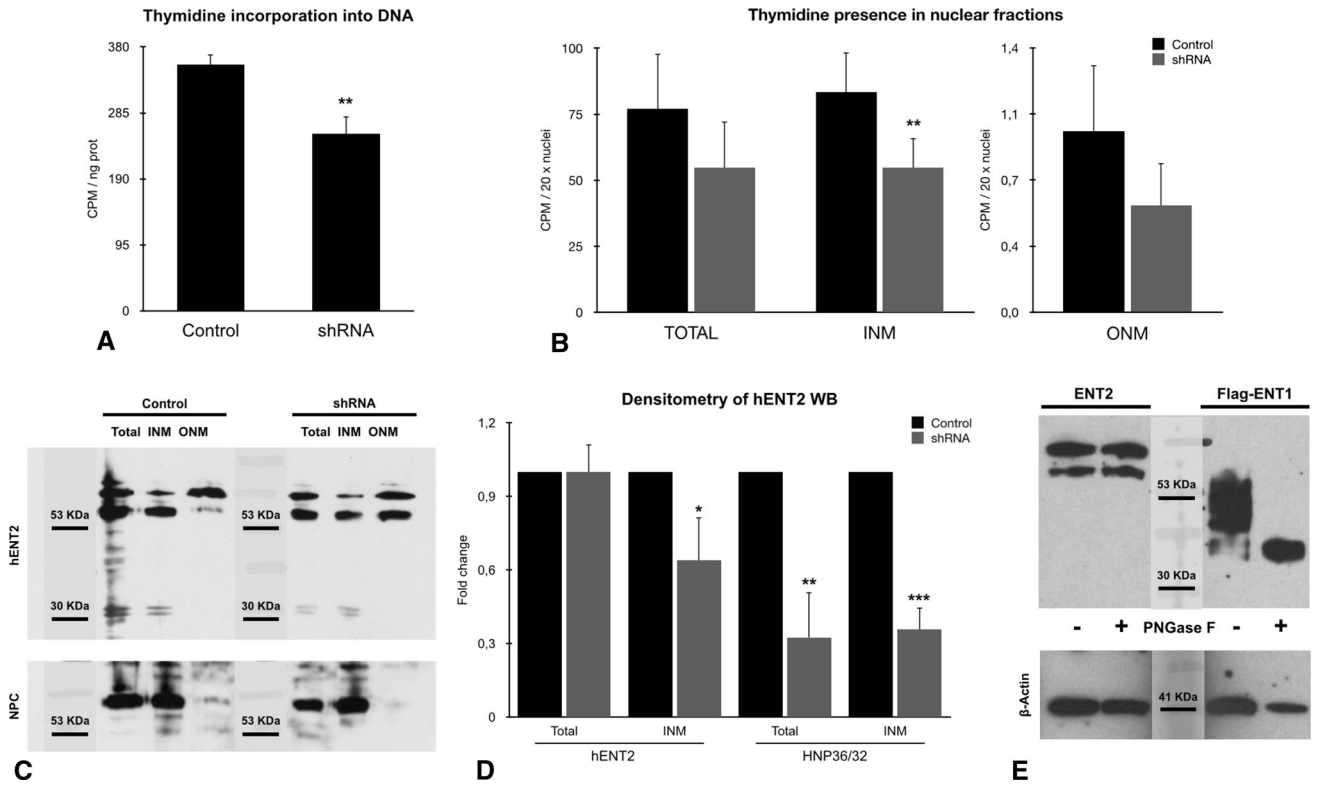

Fig. 5 Thymidine incorporation into DNA requires the participation of HNP36 and HNP32. **a** Thymidine incorporation into DNA after HNP36 and HNP32 knockdown co-transfecting both shRNA constructs 197J + 198J in HEK-293 cells (labelled as shRNA). Control samples expressed a scrambled shRNA construct. **b** Thymidine presence in isolated nuclei, INM and the nuclear lumen (ONM) fractions from HEK-293 cells. All graphs represent mean ± SEM; $n = 4$; $^{**}p < 0.01$. **c** Immunoblot of endogenous hENT2 isoforms in nuclear sub-fractions from HEK-293 cells. Nuclear pore complex (NPC) is shown as a loading control (representative image; $n = 4$). See also Figure S4. **d** Densitometry of the immunoblot of hENT2 proteins (mean ± SD; $n = 3$). $^{*}p < 0.05$, $^{**}p < 0.01$, $^{***}p < 0.001$. **e** Immunoblot of endogenous hENT2 and overexpressed Flag-hENT1 proteins from HEK-293 cells treated with (+) and without (−) PNGase F. Results showed no changes in ENT2 double band after deglycosylation whereas Flag-hENT1 proteins are reduced in size after being deglycosylated by PNGase F. β-Actin was used as loading control (representative image; $n = 3$)

cells, while thymidine levels in the INM sub-fraction showed a significant decrease (30 %) of incorporation into DNA (Fig. 6a). In contrast, thymidine levels in the lumen (ONM) showed a significant (2.2-fold) increase in arrested cells (Fig. 6b), suggesting the lumen of the NE functions as a reservoir of nucleosides when cells are not proliferating.

Associated with this reduced incorporation, levels of HNP36 and HNP32 protein also decreased significantly (75 %) in serum-deprived cells (Fig. 6c, d). Interestingly, we found no evidence for presence of WT hENT2 at the INM while the overall expression showed an increase (∼twofold), confirming the regulatory role of HNP36 and HNP32 in recruiting hENT2 to the INM. Immunoblotting also revealed a third band, whose nature remains unclear, right above the double band of full-length hENT2 in total and ONM fractions (Fig. 6c). Supporting these changes in protein expression, we observed a striking decrease in 45F splice variant (HNP32) mRNA expression levels in arrested cells, while WT hENT2 levels significantly increased (Fig. 6e). No change in expression levels of 4A and 16D splice variants was noted suggesting that 45F is the predominant variant down-regulated under non-proliferative conditions. These results confirm that the expression of hENT2 splice variants is highly regulated depending on the proliferative state of the cell. Furthermore, since a decrease in HNP32 implied an increase in hENT2 expression, the mechanism involved in such regulation most likely implies specific splicing factors that generate either WT hENT2 or its nuclear splice variants based on the needs of the cell.

Discussion

The mechanisms controlling cell division and tissue growth are well known [1–3]. However, very basic metabolic events, such as those determining the supply of nucleotides for DNA replication are far less understood. Here, we provide evidence supporting a novel role for members of the SLC29 family of proteins in the regulation of cell proliferation. In our model, HNP36 and HNP32 act to

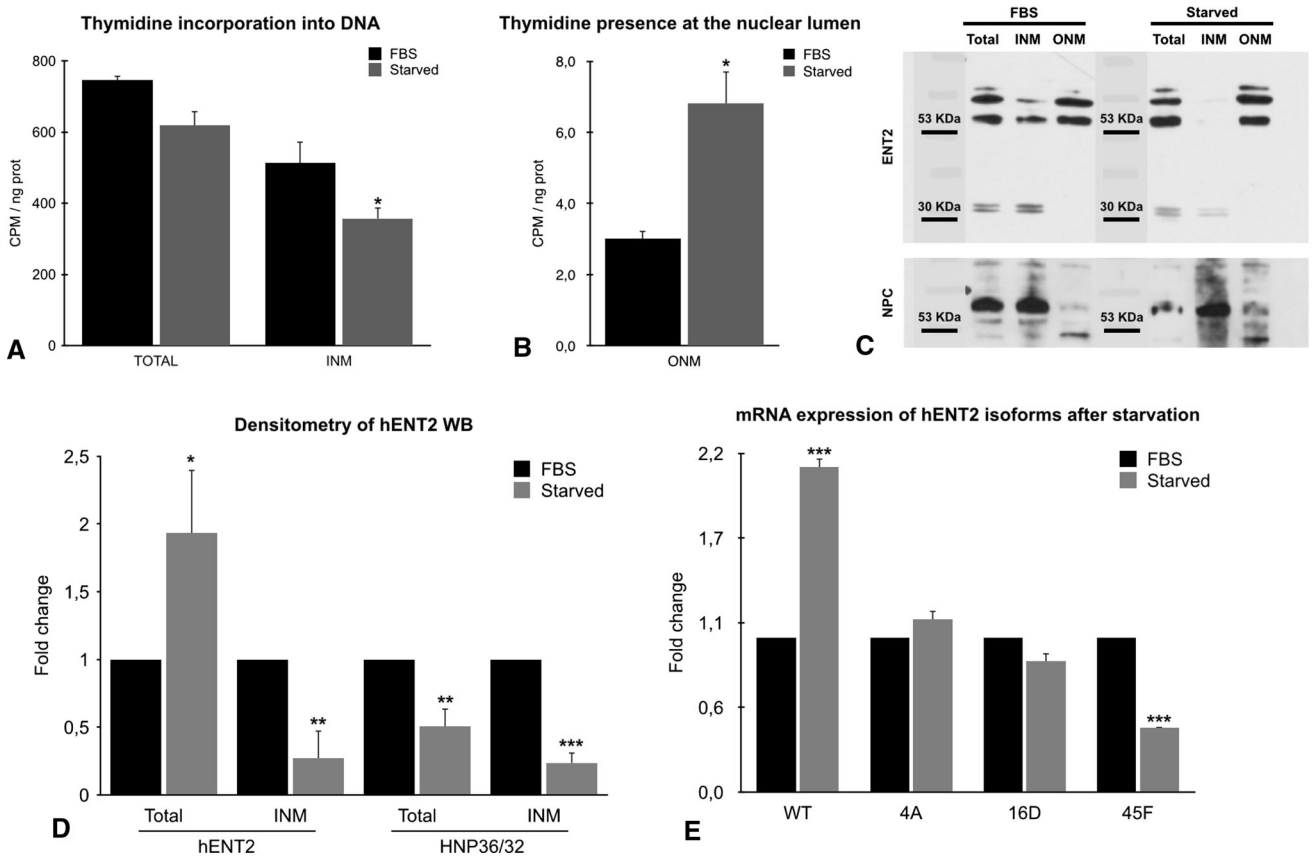

Fig. 6 Regulation of HNP36 and HNP32 after cell starvation in HEK-293 cells. **a** Decrease of thymidine incorporation into DNA after cell starvation in isolated nuclei and INM sub-fraction. **b** Significant increase of presence of thymidine in the nuclear lumen (ONM sub-fraction) after cell starvation. All graphs represent mean ± SEM; $n = 4$; $*p < 0.05$, $***p < 0.001$. **c** Immunoblot of endogenous hENT2 isoforms in isolated nuclei, INM and ONM sub-fractions after cell starvation. Nuclear pore complex (NPC) is shown as a loading control (representative image; $n = 4$). **d** Densitometry of the immunoblot of hENT2 proteins (mean ± SD; $n = 3$). $*p < 0.05$, $**p < 0.01$, $***p < 0.001$. **e** mRNA expression of hENT2 isoforms after cell starvation

localise hENT2 at the INM where they form functional heteromers that supply nucleosides necessary for DNA replication into the nucleus.

Oligomerisation of hENT2 and sorting to the NE

HNP36 was reported to be located at the NE [17] although the functional significance of this observation has been unclear for many years. We have confirmed this observation and significantly extended it by demonstrating that HNP36 and HNP32 are present at the INM. However, the mechanism underlaying the sorting of these splice variants to the NE remains unclear. It has been previously reported that trafficking of hENT2 to the plasma membrane can be affected by glycosylation [48] and, therefore, the localisation of these variants to the nuclear membrane could be due to the lack of TM1 which leads to the loss of glycosylation sites, Asn48 and Asn57, thereby affecting intracellular sorting without affecting function. Our results did not confirm the role of glycosylation in the trafficking of full-length hENT2 to the INM; therefore, further studies should be conducted to understand the mechanism underlying the differential sorting of hENT2 proteins.

HNP36 and HNP32 are the first splice variants confirmed as functional transporters for any human ENT member, and they regulate the WT isoform both in terms of biological function and sub-cellular localisation [12, 14]. Alternative splice variants often inhibit and/or modulate a WT protein through PPI and the formation of heteromers [49–51]. It is also well known that oligomerisation works as a mechanism for the stabilisation and regulation of a large number of transmembrane proteins, including transporters [46, 52–55]. It is currently unknown whether oligomerisation of ENTs occurs, although recent studies described the crystal structure of a CNT in *Vibrio cholerae* as a trimer and proposed the formation of oligomers for the human ortholog [56]. Our results are the first, to our knowledge, that demonstrate the existence of PPI among different isoforms of hENT2 and that suggest the formation of heteromers among species of hENT2 along with their

co-localisation at the NE. This hetero-oligomerisation appears to be part of the mechanism that regulates the sorting of hENT2, by recruiting it to the INM, and hence decreasing hENT2-mediated transport activity at the plasma membrane. In conclusion, HNP32 and HNP36 act as dominant negatives of WT hENT2 at the plasma membrane, although these proteins appear to form functional oligomers at the INM which are capable of internalising nucleosides and nucleobases into the nucleus.

Role of hENT2 oligomers at the NE

Our results demonstrate the presence of functional nucleoside transporters at the NE raising questions as to their role and the relevance of nucleosides in the nucleus.

The NE comprises the outer nuclear membrane (ONM) and the inner nuclear membrane (INM) joined at the nuclear pore complex (NPC), generating an inter-membrane space or lumen that acts as a calcium store surrounding the nucleus [57, 58]. Here, we propose a novel model for nucleoside compartmentalisation at the NE allowing for rapid release to the nucleus under mitogenic conditions (Fig. 7). Based on our results, the presence of hENT2 heteromers at the INM would help transport nucleosides from the lumen into the nucleus under proliferative conditions. A functional model concentrating nucleosides at the NE would also require the presence of a concentrative transporter (hCNT) at the ONM, which would transport nucleosides against a concentration gradient. Indeed, previous work from our laboratory describes a functional hCNT3 variant (hCNT3ins) which is localised at the ER [59]. The ER has a contiguous membrane with the ONM and shares the lumen space with the NE. Therefore, we propose a model in which ER-located hCNT3ins concentrates nucleosides in the lumen space of the NE. Subsequently, under mitogenic conditions, HNP36 and HNP32 are up-regulated and recruit hENT2 to the INM to enhance the flux of nucleosides into the nucleoplasm enabling efficient DNA synthesis. Furthermore, hCNT3ins is a concentrative transporter which co-transports sodium cations into the lumen space. These ions can be transported into the nucleoplasm by a sodium–calcium exchanger (NCX) which is located at the INM to preserve the calcium store in the NE [60–62].

Interestingly, a similar mechanism has been previously described in plants, where nucleobases and nucleosides are released from storage organelles during germination and then recycled by the salvage pathway [63]. Similarly, several studies in mammalian cells describe the existence of two different nucleotide pools within the cell, one in the cytosol and one at the nucleus [21]. These nucleotide pools have been reported to be in disequilibrium with each other, in such a way that the concentration of nucleotides in the nuclear pool increased to micromolar concentrations when cells entered S phase of cell cycle to support DNA replication [20, 22]. Taken together, these studies support the existence of a regulated mechanism of transport and storage of nucleotides at the nucleus which facilitates the rapid

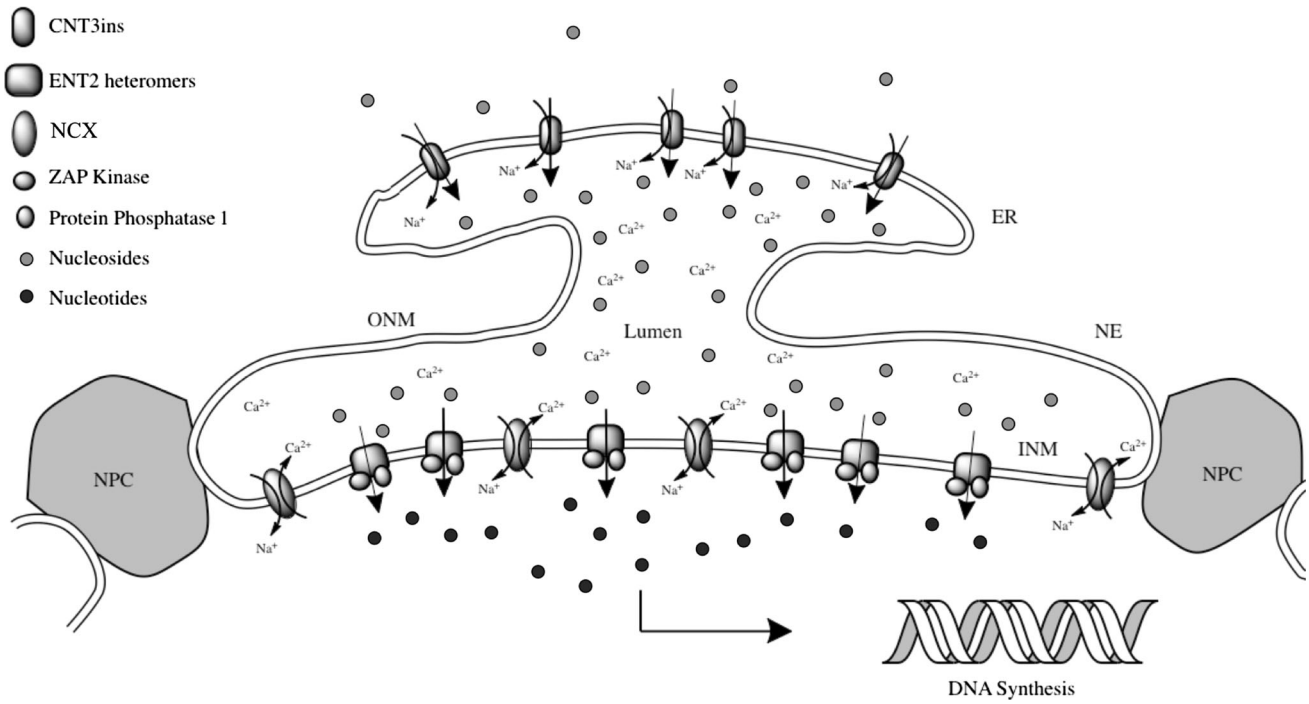

Fig. 7 Proposed model for the role of nucleoside transporters and compartmentalisation of nucleosides at the NE. Cartoon representing the NE and its INM and ONM, as well as hENT2 nuclear variants located at the INM to translocate nucleosides from the lumen into the nucleoplasm

release of nucleotides into the nucleoplasm to synthesise DNA. This model (Fig. 7) is consistent with our results showing changes in cell cycle with decreased HNP36 and HNP32 expression as a consequence of reduced nucleoside translocation into the nucleus. Moreover, our model is also supported by previous studies which demonstrated that a reduction in levels of nucleotides leads to DNA damage and genome instability due to a slow replication fork progression during DNA replication and a dysregulation of cell cycle resulting in an increase in the percentage of cells in S phase [7, 8], coinciding with our observations after knocking down the expression of HNP36 and HNP32.

Most recent studies on chromosome replication have focused on the machinery necessary for DNA synthesis, assuming that when a cell enters S phase of the cell cycle, there are always sufficient levels of nucleotides in the nucleus to replicate the whole chromosome. Nucleoside to nucleotide metabolism has been reported as taking place in the cytosol with translocation of nucleotides into the nucleus through the non-specific NPC being inferred [63–65]. However, it is very unlikely that sufficient levels of nucleosides/nucleotides are present in the cytoplasm indefinitely without metabolism, and thus will become a limiting factor for DNA synthesis and subsequent cell duplication. In contrast, the presence of a number of key nucleoside metabolic enzymes within the nucleus suggests that nucleoside to nucleotide metabolism occurs in this location and that a supply of nucleosides to feed this metabolic process will exist [66–70]. Intriguingly, we recently identified protein phosphatase 1 (PP1) in a MYTH screen [71] as a putative interacting protein of hENT2 (unpublished data) and it was also recently reported that the novel nucleoside kinase ZAP, which is localised at the nucleus, also interacts with PP1 [70]. An interaction between ZAP-PP1 and PP1-hENT2 would bring ZAP and hENT2 together in a metabolon to enable nucleosides delivered by hENT2 to be rapidly metabolised to nucleotides by ZAP and then incorporated into the newly synthesised DNA chains (Fig. 7). Thus, we believe that our data, along with newly identified components of nucleoside metabolism in the nucleus, point to a novel and previously unidentified metabolic machinery that is present very close to location of DNA synthesis.

Therapeutic implications

hENT2 is a marker for advanced stages of cancer [72] and elevated hENT2 expression is correlated with vascular invasion and poorer outcomes in various models (hepatocellular carcinoma, mantle cell lymphoma and ovarian carcinoma) [73, 74]. Our findings contribute to understand why cancer cells, with an enhanced expression of nuclear hENT2 isoforms, have a substantial availability of nucleotides to facilitate cellular proliferation. Furthermore, hENT2 plays a crucial role as a nucleoside-derived anticancer drug transporter, especially in the case of chronic lymphocytic leukaemia (CLL) [75, 76]. Therefore, CLL cells expressing high levels of HNP36/32 proteins would be less affected by anticancer nucleoside analogs since these cells would have a decreased capacity to transport nucleoside-derived drugs inside the cell due to a reduced presence of WT hENT2 at the plasma membrane.

It is well known that alternative splicing is drastically altered in cancer cells to support cellular proliferation [37–40]. Recent studies have identified a large number of molecules and treatments that modify the alternative splicing pattern in different cancer models [77, 78]. Consequently, alternative splicing has become a new target for cancer therapy. A deeper understanding of regulation of alternative splicing of hENT2 could enable a therapeutic reversion of the ratio of WT/nuclear isoforms. Therefore, further studies should identify molecules and treatments to modify the splicing pattern of hENT2 in cancer cells to promote the expression of WT hENT2 to increase drug uptake and also deprive the proliferative cell from a critical pool of nucleosides within the nucleus.

Acknowledgments This work was supported by La Obra Social "La Caixa", Spain (masters fellowship); Instituto de Salud Carlos III, Spain (PFIS doctoral fellowship); Ryerson University, Canada (Postdoctoral fellowship) to NGB; the Natural Science and Engineering Research Council (NSERC) of Canada; Ryerson University to IRC; the Ministry of Economy and Competitiveness (Plan Nacional de Biomedicina—MINECO), Government of Spain (SAF2011-23660 and SAF2014-52067-R); National Biomedical Research Institute of Liver and Gastrointestinal Diseases (CIBER EHD) to MPA. CIBER is an initiative of Instituto de Salud Carlos III, Spain.

References

1. Bertoli C, Skotheim JM, de Bruin RAM (2013) Control of cell cycle transcription during G1 and S phases. Nat Rev Mol Cell Biol 14:518–528. doi:10.1038/nrm3629
2. Golias CH, Charalabopoulos A, Charalabopoulos K (2004) Cell proliferation and cell cycle control: a mini review. Int J Clin Pract 58:1134–1141. doi:10.1111/j.1368-5031.2004.00284.x
3. Massagué J (2004) G1 cell-cycle control and cancer. Nature 432:298–306. doi:10.1038/nature03094
4. Alabert C, Groth A (2012) Chromatine replication and epigenome maintenance. Nat Rev Mol Cell Biol 13:153–167. doi:10.1038/nrm3288
5. Kelly TJ, Brown GW (2000) Regulation of chromosome replication. Annu Rev Biochem 69:829–880. doi:10.1146/annurev.biochem.69.1.829
6. McCulloch SD, Kunkel TA (2008) The fidelity of DNA synthesis by eukaryotic replicative and translesion synthesis polymerases. Cell Res 18:148–161. doi:10.1038/cr.2008.4
7. Anglana M, Apiou F, Bensimon A, Debatisse M (2003) Dynamics of DNA replication in mammalian somatic cells. Cell 114:385–394. doi:10.1016/S0092-8674(03)00569-5
8. Bester AC, Roniger M, Oren YS et al (2011) Nucleotide deficiency promotes genomic instability in early stages of cancer development. Cell 145:435–446. doi:10.1016/j.cell.2011.03.044

9. Cabrita MA, Baldwin SA, Young JD, Cass CE (2002) Molecular biology and regulation of nucleoside and nucleobase transporter proteins in eukaryotes and prokaryotes. Biochem Cell Biol 80:623–638
10. Rose JB, Coe IR (2008) Physiology of nucleoside transporters: back to the future. Physiology (Bethesda) 23:41–48. doi:10.1152/physiol.00036.2007
11. Yegutkin GG (2008) Nucleotide- and nucleoside-converting ectoenzymes: important modulators of purinergic signalling cascade. Biochim Biophys Acta 1783:673–694. doi:10.1016/j.bbamcr.2008.01.024
12. Molina-Arcas M, Casado FJ, Pastor-Anglada M (2009) Nucleoside transporter proteins. Curr Vasc Pharmacol 7:426–434
13. dos Santos-Rodrigues A, Grañe-Boladeras N, Bicket A, Coe IR (2014) Nucleoside transporters in the purinome. Neurochem Int 73:229–237. doi:10.1016/j.neuint.2014.03.014
14. Young JD, Yao SYM, Baldwin JM et al (2013) The human concentrative and equilibrative nucleoside transporter families, SLC28 and SLC29. Mol Aspects Med 34:529–547. doi:10.1016/j.mam.2012.05.007
15. Endo Y, Obata T, Murata D et al (2007) Cellular localization and functional characterization of the equilibrative nucleoside transporters of antitumor nucleosides. Cancer Sci 98:1633–1637. doi:10.1111/j.1349-7006.2007.00581.x
16. Griffiths M, Beaumont N, Yao SYM et al (1997) Cloning of a human nucleoside transporter implicated in the cellular uptake of adenosine and chemotherapeutic drugs. Nat Med 3:89–93
17. Williams JB, Lanahan AA (1995) A mammalian delayed-early response gene encodes HNP36, a novel, conserved nucleolar protein. Biochem Biophys Res Commun 213:325–333. doi:10.1006/bbrc.1995.2133
18. Crawford CR, Patel DH, Naeve C, Belt JA (1998) Cloning of the human equilibrative, nitrobenzylmercaptopurine riboside (NBMPR)-insensitive nucleoside transporter ei by functional expression in a transport-deficient cell line. J Biol Chem 273:5288–5293
19. Mani RS, Hammond JR, Marjan JM et al (1998) Demonstration of equilibrative nucleoside transporters (hENT1 and hENT2) in nuclear envelopes of cultured human choriocarcinoma (BeWo) cells by functional reconstitution in proteoliposomes. J Biol Chem 273:30818–30825
20. Bjursell G, Skoog L (1979) Control of nucleotide pools in mammalian cells. Antibiot Chemother 20:78–85
21. Khym JX, Jones MH, Lee WH et al (1978) On the question of compartmentalization of the nucleotide pool. J Biol Chem 253:8741–8746
22. Plagemann PG (1972) Nucleotide pools in Novikoff rat hepatoma cells growing in suspension culture. 3. Effects of nucleosides in medium on levels of nucleotides in separate nucleotide pools for nuclear and cytoplasmic RNA synthesis. J Cell Biol 52:131–146
23. Chang Y-F, Imam JS, Wilkinson MF (2007) The nonsense-mediated decay RNA surveillance pathway. Annu Rev Biochem 76:51–74. doi:10.1146/annurev.biochem.76.050106.093909
24. Boutz PL, Stoilov P, Li Q et al (2007) A post-transcriptional regulatory switch in polypyrimidine tract-binding proteins reprograms alternative splicing in developing neurons. Genes Dev 21:1636–1652. doi:10.1101/gad.1558107
25. Guillén-Gómez E, Pinilla-Macua I, Pérez-Torras S et al (2012) New role of the human equilibrate nucleoside transporter 1 (hENT1) in epithelial-to-mesenchymal transition in renal tubular cells. J Cell Physiol 227:1521–1528
26. Yao SYM, Ng AM, Sundaram M et al (2001) Transport of antiviral 3′-deoxy-nucleoside drugs by recombinant human and rat equilibrative, nitrobenzylthioinosine (NBMPR)-insensitive (ENT2) nucleoside transporter proteins produced in *Xenopus* oocytes. Mol Membr Biol 18:161–167
27. Baldwin SA, Yao SYM, Hyde RJ et al (2005) Functional characterization of novel human and mouse equilibrative nucleoside transporters (hENT3 and mENT3) located in intracellular membranes. J Biol Chem 280:15880–15887. doi:10.1074/jbc.M414337200
28. Govindarajan R, Leung GPH, Zhou M et al (2009) Facilitated mitochondrial import of antiviral and anticancer nucleoside drugs by human equilibrative nucleoside transporter-3. Am J Physiol Gastrointest Liver Physiol 296:G910–G922. doi:10.1152/ajpgi.90672.2008
29. Quah BJC, Parish CR (2010) The use of carboxyfluorescein diacetate succinimidyl ester (CFSE) to monitor lymphocyte proliferation. J Vis Exp. doi:10.3791/2259
30. Darzynkiewicz Z, Juan G, Bedner E (2001) Determining cell cycle stages by flow cytometry. Curr Protoc Cell Biol Chapter 8:Unit 8.4. doi:10.1002/0471143030.cb0804s01
31. Xaus J, Cardó M, Valledor AF et al (1999) Interferon gamma induces the expression of p21waf-1 and arrests macrophage cell cycle, preventing induction of apoptosis. Immunity 11:103–113
32. Gilchrist JS, Pierce GN (1993) Identification and purification of a calcium-binding protein in hepatic nuclear membranes. J Biol Chem 268:4291–4299
33. Rosner M, Schipany K, Hengstschläger M (2013) Merging high-quality biochemical fractionation with a refined flow cytometry approach to monitor nucleocytoplasmic protein expression throughout the unperturbed mammalian cell cycle. Nat Protoc 8:602–626. doi:10.1038/nprot.2013.011
34. Mangravite LM, Xiao G, Giacomini KM (2003) Localization of human equilibrative nucleoside transporters, hENT1 and hENT2, in renal epithelial cells. Am J Physiol Renal Physiol 284:F902–F910. doi:10.1152/ajprenal.00215.2002
35. Valdés R, Elferich J, Shinde U, Landfear SM (2014) Identification of the intracellular gate for a member of the equilibrative nucleoside transporter (ENT) family. J Biol Chem 289:8799–8809. doi:10.1074/jbc.M113.546960
36. Valdés R, Vasudevan G, Conklin D, Landfear SM (2004) Transmembrane domain 5 of the LdNT1.1 nucleoside transporter is an amphipathic helix that forms part of the nucleoside translocation pathway. Biochemistry 43:6793–6802. doi:10.1021/bi049873m
37. Al-Ayoubi AM, Zheng H, Liu Y et al (2012) Mitogen-activated protein kinase phosphorylation of splicing factor 45 (SPF45) regulates SPF45 alternative splicing site utilization, proliferation, and cell adhesion. Mol Cell Biol 32:2880–2893. doi:10.1128/MCB.06327-11
38. Das S, Anczuków O, Akerman M, Krainer AR (2012) Oncogenic splicing factor SRSF1 is a critical transcriptional target of Myc. Cell Rep 1:110–117. doi:10.1016/j.celrep.2011.12.001
39. Tazi J, Bakkour N, Stamm S (2009) Alternative splicing and disease. Biochim Biophys Acta 1792:14–26. doi:10.1016/j.bbadis.2008.09.017
40. Venables JP, Klinck R, Koh C et al (2009) Cancer-associated regulation of alternative splicing. Nat Struct Mol Biol 16:670–676. doi:10.1038/nsmb.1608
41. Stamm S, Ben-Ari S, Rafalska I et al (2005) Function of alternative splicing. Gene 344:1–20. doi:10.1016/j.gene.2004.10.022
42. Chiu YH, Alvarez-Baron C, Kim EY, Dryer SE (2010) Dominant-negative regulation of cell surface expression by a pentapeptide motif at the extreme COOH terminus of an Slo1 calcium-activated potassium channel splice variant. Mol Pharmacol 77:497–507. doi:10.1124/mol.109.061929
43. Dabertrand F, Morel J-L, Sorrentino V et al (2006) Modulation of calcium signalling by dominant negative splice variant of ryanodine receptor subtype 3 in native smooth muscle cells. Cell Calcium 40:11–21. doi:10.1016/j.ceca.2006.03.008
44. Leung P-K, Chow KBS, Lau P-N et al (2007) The truncated ghrelin receptor polypeptide (GHS-R1b) acts as a dominant-

negative mutant of the ghrelin receptor. Cell Signal 19:1011–1022. doi:10.1016/j.cellsig.2006.11.011
45. Veale EL, Rees KA, Mathie A, Trapp S (2010) Dominant negative effects of a non-conducting TREK1 splice variant expressed in brain. J Biol Chem 285:29295–29304. doi:10.1074/jbc.M110.108423
46. Mo W, Zhang J-T (2009) Oligomerization of human ATP-binding cassette transporters and its potential significance in human disease. Expert Opin Drug Metab Toxicol 5:1049–1063. doi:10.1517/17425250903124371
47. Vickers MF, Mani RS, Sundaram M et al (1999) Functional production and reconstitution of the human equilibrative nucleoside transporter (hENT1) in Saccharomyces cerevisiae. Interaction of inhibitors of nucleoside transport with recombinant hENT1 and a glycosylation-defective derivative (hENT1/N48Q). Biochem J 339(Pt 1):21–32
48. Ward JL, Leung GPH, Toan S-V, Tse C-M (2003) Functional analysis of site-directed glycosylation mutants of the human equilibrative nucleoside transporter-2. Arch Biochem Biophys 411:19–26. doi:10.1016/S0003-9861(02)00718-X
49. Brueggemann LI, Mackie AR, Cribbs LL et al (2014) Differential protein kinase C-dependent modulation of Kv7.4 and Kv7.5 subunits of vascular Kv7 channels. J Biol Chem 289:2099–2111. doi:10.1074/jbc.M113.527820
50. Mary S, Fehrentz JA, Damian M et al (2013) Heterodimerization with its splice variant blocks the ghrelin receptor 1a in a non-signaling conformation: a study with a purified heterodimer assembled into lipid discs. J Biol Chem 288:24656–24665. doi:10.1074/jbc.M113.453423
51. Poeppel P, Abouzied MM, Völker C, Gieselmann V (2010) Misfolded endoplasmic reticulum retained subunits cause degradation of wild-type subunits of arylsulfatase A heteromers. FEBS J 277:3404–3414. doi:10.1111/j.1742-4658.2010.07745.x
52. Cymer F, Schneider D (2012) Oligomerization of polytopic α-helical membrane proteins: causes and consequences. Biol Chem 393:1215–1230
53. Kilic F, Rudnick G (2000) Oligomerization of serotonin transporter and its functional consequences. Proc Natl Acad Sci USA 97:3106–3111. doi:10.1073/pnas.060408997
54. Raja M (2011) The potassium channel KcsA: a model protein in studying membrane protein oligomerization and stability of oligomeric assembly? Arch Biochem Biophys 510:1–10. doi:10.1016/j.abb.2011.03.010
55. Torres GE (2002) Oligomerization and trafficking of the human dopamine transporter. J Biol Chem 278:2731–2739. doi:10.1074/jbc.M201926200
56. Johnson ZL, Cheong C-G, Lee S-Y (2012) Crystal structure of a concentrative nucleoside transporter from *Vibrio cholerae* at 2.4 Å. Nature 483:489–493. doi:10.1038/nature10882
57. Mauger J-P (2011) Role of the nuclear envelope in calcium signalling. Biol Cell 104:70–83. doi:10.1111/boc.201100103
58. Petersen OH, Gerasimenko OV, Gerasimenko JV et al (1998) The calcium store in the nuclear envelope. Cell Calcium 23:87–90
59. Errasti-Murugarren E, Molina-Arcas M, Casado FJ, Pastor-Anglada M (2009) A splice variant of the SLC28A3 gene encodes a novel human concentrative nucleoside transporter-3 (hCNT3) protein localized in the endoplasmic reticulum. FASEB J 23:172–182. doi:10.1096/fj.08-113902
60. Ledeen RW, Wu G (2007) Sodium–calcium exchangers in the nucleus: an unexpected locus and an unusual regulatory mechanism. Ann N Y Acad Sci 1099:494–506. doi:10.1196/annals.1387.057
61. Wu G, Xie X, Lu Z-H, Ledeen RW (2009) Sodium–calcium exchanger complexed with GM1 ganglioside in nuclear membrane transfers calcium from nucleoplasm to endoplasmic reticulum. Proc Natl Acad Sci USA 106:10829–10834. doi:10.1073/pnas.0903408106
62. Xie X, Wu G, Lu Z-H, Ledeen RW (2002) Potentiation of a sodium–calcium exchanger in the nuclear envelope by nuclear GM1 ganglioside. J Neurochem 81:1185–1195
63. Moffatt BA, Ashihara H (2002) Purine and pyrimidine nucleotide synthesis and metabolism. Arabidopsis Book 39:1. doi:10.1199/tab.0018
64. An S, Kumar R, Sheets ED, Benkovic SJ (2008) Reversible compartmentalization of de novo purine biosynthetic complexes in living cells. Science 320:103–106. doi:10.1126/science.1152241
65. Jones ME (1980) Pyrimidine nucleotide biosynthesis in animals: genes, enzymes, and regulation of UMP biosynthesis. Annu Rev Biochem 49:253–279
66. Lenger K (1982) Characterization of six nucleoside-nucleotide phosphotransferases from the chromatin of Morris hepatoma 9121 cells by physicochemical and biochemical techniques. Int J Biochem 14:955–960
67. Lenger K (1982) Isolation of nucleoside phosphotransferases from chromatin of Morris hepatoma 9121 nuclei. Int J Biochem 14:53–61
68. Johansson M, Brismar S, Karlsson A (1997) Human deoxycytidine kinase is located in the cell nucleus. Proc Natl Acad Sci USA 94:11941–11945
69. Sigoillot FD, Kotsis DH, Serre V et al (2005) Nuclear localization and mitogen-activated protein kinase phosphorylation of the multifunctional protein CAD. J Biol Chem 280:25611–25620. doi:10.1074/jbc.M504581200
70. Ulke-Lemée A, Trinkle-Mulcahy L, Chaulk S et al (2007) The nuclear PP1 interacting protein ZAP3 (ZAP) is a putative nucleoside kinase that complexes with SAM68, CIA, NF110/45, and HNRNP-G. Biochim Biophys Acta 1774:1339–1350. doi:10.1016/j.bbapap.2007.07.015
71. Snider J, Kittanakom S, Damjanovic D et al (2010) Detecting interactions with membrane proteins using a membrane two-hybrid assay in yeast. Nat Protoc 5:1281–1293. doi:10.1038/nprot.2010.83
72. Hartmann E, Fernàndez V, Moreno V et al (2008) Five-gene model to predict survival in mantle-cell lymphoma using frozen or formalin-fixed, paraffin-embedded tissue. J Clin Oncol 26:4966–4972. doi:10.1200/JCO.2007.12.0410
73. Bock AJ, Dong HP, Tropé CG et al (2011) Nucleoside transporters are widely expressed in ovarian carcinoma effusions. Cancer Chemother Pharmacol 69:467–475. doi:10.1007/s00280-011-1716-7
74. Chen C-F, Hsu E-C, Lin K-T et al (2010) Overlapping high-resolution copy number alterations in cancer genomes identified putative cancer genes in hepatocellular carcinoma. Hepatology 52:1690–1701. doi:10.1002/hep.23847
75. Molina-Arcas M, Bellosillo B, Casado FJ et al (2003) Fludarabine uptake mechanisms in B-cell chronic lymphocytic leukemia. Blood 101:2328–2334. doi:10.1182/blood-2002-07-2236
76. Pastor-Anglada M, Molina-Arcas M, Casado FJ et al (2004) Nucleoside transporters in chronic lymphocytic leukaemia. Leukemia 18:385–393. doi:10.1038/sj.leu.2403271
77. Hagiwara M (2005) Alternative splicing: a new drug target of the post-genome era. Biochim Biophys Acta 1754:324–331. doi:10.1016/j.bbapap.2005.09.010
78. Sumanasekera C, Watt DS, Stamm S (2008) Substances that can change alternative splice-site selection. Biochem Soc Trans 36:483–490. doi:10.1042/BST0360483